


RESEARCH

Open Access



# Bladder involvement in placenta accreta spectrum disorders: 2D US combined with the 3D crystal Vue and MRI comparative analysis

Xiufang Shuai<sup>1</sup>, Chuanfen Gao<sup>1</sup>, Hanqi Zhang<sup>1</sup>, Tingting Zhang<sup>2</sup>, Hongwen Li<sup>2</sup>, Yunfang Yan<sup>3</sup>, Wen Yao<sup>1</sup>, Yu Liu<sup>1</sup> and Chaoxue Zhang<sup>1\*</sup> 

## Abstract

**Background** Placental accreta spectrum (PAS) disorder with bladder involvement is found to be associated with severe maternal and neonatal morbidity. When planning surgery or other treatments, a diagnosis and assessment of the invasiveness of placenta accreta spectrum disorder with bladder involvement are crucial. The detection of the depth of villi invasion can be accomplished with both MRI and US. The advent of three-dimensional Crystal Vue provides details additional information for scanning abnormal issue.

**Purpose** Our goal was to compare and assess the diagnostic accuracy of 2D US combined with the 3D Crystal Vue and MRI in case of placenta accreta spectrum (PAS) involving the bladder.

**Materials and methods** 111 pregnancy patients between May 2019 and November 2023 at the First Affiliated Hospital of Anhui Medical University whether or not they had placenta previa were included in the study if they were diagnosed of having placenta increta (PI) or placenta percreta (PP). Both US and MRI were used to evaluate the pregnant women. Total 53 pregnant women were ultimately included in our analysis. 53 patients were split into groups with and without bladder involvement. They underwent 2D US, 3D Crystal Vue, and MRI. The visual features of every subject were noted. Next, we analyzed the fundamental information, associated medical history, pregnancy outcomes, and different US and MRI signals between the two groups. To determine the potential contributing factors of PAS complicated with bladder involvement, a univariate analysis was performed. A multivariable logistic regression analysis was performed to identify US and MRI findings predictive of bladder involvement in placenta accreta spectrum.

**Results** Multiple logistic regression analysis found that the bridging vessels (OR, 31.76, 95% CI, 1.64–614.31,  $p=0.022$ ) and the tramline sign “fully” obliterated on Crystal Vue feature (OR, 68.92; 95% CI, 6.76–702.35,  $p<0.001$ ) were independently associated with an increased likelihood of bladder involvement. These findings when combined allowed for the prediction of bladder involvement with an 88.2% sensitivity, a 94.4% specificity, and an AUC of 0.933 (95% CI, 0.829–0.983,  $p=0.001$ ). The results of the MRI logistic regression analysis were as follows: the three independent risk factors for bladder involvement were: Placental bulge (OR, 57.99, 95% CI, 3.89–835.80,  $p=0.003$ ), Bladder

\*Correspondence:  
Chaoxue Zhang  
zcxay@163.com

Full list of author information is available at the end of the article



© The Author(s) 2024. **Open Access** This article is licensed under a Creative Commons Attribution-NonCommercial-NoDerivatives 4.0 International License, which permits any non-commercial use, sharing, distribution and reproduction in any medium or format, as long as you give appropriate credit to the original author(s) and the source, provide a link to the Creative Commons licence, and indicate if you modified the licensed material. You do not have permission under this licence to share adapted material derived from this article or parts of it. The images or other third party material in this article are included in the article's Creative Commons licence, unless indicated otherwise in a credit line to the material. If material is not included in the article's Creative Commons licence and your intended use is not permitted by statutory regulation or exceeds the permitted use, you will need to obtain permission directly from the copyright holder. To view a copy of this licence, visit <http://creativecommons.org/licenses/by-nc-nd/4.0/>.

wall interruption (OR, 11.93, 95%CI, 1.60–88.85,  $p=0.016$ ), and Bladder vessel sign (OR, 9.75, 95%CI, 1.43–66.21,  $p=0.020$ ). The joint diagnosis showed a sensitivity of 94.1% and specificity of 83.3%. The area under the curve was 0.942 (95%CI, 0.841–0.988). Regarding projected bladder involvement, there were no statistically significant differences between MRI and 2D integrated 3D Crystal Vue imaging.

**Conclusion** Both 2D coupled 3D Crystal Vue imaging and MRI are highly effective for predicting bladder invasion. Ultrasound is preferred over MRI because it is more convenient and more affordable. Among them, the tramline sign “fully” obliterated on 3D Crystal Vue was a new and reliable US sign for detecting bladder involvement.

**Keywords** Placenta accreta spectrum, Crystal Vue, Magnetic resonance imaging

## Introduction

In order to replace the terms abnormally adherent/invasive placenta and morbidly adherent placenta, the International Federation of Obstetrics and Gynecology (FIGO) recommended a term called placenta accreta spectrum [1]. This spectrum includes three types of placenta: placenta accrete (PA), placenta increta (PI), and placenta percreta (PP) [2]. If the placental villi are only in contact with the myometrium, the condition is referred to as “PA.” If the villi penetrate into the myometrium, the condition is now called “PI.” If the villi invade the uterine serosa or through to the parametrial, it is referred to as “PP.” According to the 2019 Federation of Gynecology and Obstetrics (FIGO) clinical classification [3] for deep myometrial invasion, three grades make up the PAS. FIGO 1 (Grade 1): Abnormally adherent placenta (placenta adherenta or creta, PA), FIGO 2 (Grade 2): Abnormally invasive placenta (Increta, PI), FIGO 3 (Grade 3): Abnormally invasive placenta (Percreta, PP). In the FIGO system [3], Three subtypes (3a, 3b, and 3c) found in FIGO 3 (Grade 3) based on the location of invasion. FIGO 3a show invasion limited by the uterine serosa, FIGO 3b shows urinary bladder invasion, and FIGO 3c shows invasion of other pelvic tissues/organs. The only methods to arrive at a conclusive diagnosis are histopathology or clinical diagnosis.

The overall reported incidence of PAS incidence varies between 1.7 per 10,000 deliveries (based on A National Case-Control Study in the UK [4]) and 90 per 10,000 deliveries (based on A Survey of 310 Cases in an Israeli [5]). The reported incidence of PAS is affected by variations in study designs, diagnostic criteria, and statistical populations [5–8]. A systematic review and meta-analysis [8] found that retrospective studies showed a 2-fold increase in PAS incidence compared to prospective studies, and in comparison with national and international studies, there was a 3- to 5-fold increase in institutions, network, and regional reports which usually involve centers that specialize in treating and diagnosing PAS [8]. Although the reported incidence rates differ greatly, PAS has steadily increased over the years [9]. In recent years, PAS has been a major worry due to its potential to produce severe postpartum hemorrhage and to exacerbate a

number of perinatal problems [10–12]. Because the bladder is closest to the uterus, it is most frequently involved in placenta percreta. Individuals with bladder invasion are more likely to experience life threatening hemorrhage, ureteral damage [13–15]. As a result, bladder invasion prolongs hospital stays and surgical times and is associated with high medical costs. A multidisciplinary approach is required in cases of PP involving bladder invasion, and the urologist should be consulted from the outset of the decision-making process [13, 16]. There is growing recognition of the importance of comprehensive imaging evaluation. Early diagnosis of bladder involvement in PAS is crucial for reducing severe complications and mortality.

US is the most appropriate imaging method for PAS screenings and should be the first choice due to its widespread use and relative affordability. Recent studies have demonstrated that 3D US can be used as a supplement to 2D US, providing additional information for scanning abnormal issue [17, 18]. There is evidence that 3D power Doppler improves prenatal diagnosis or excludes PAS in some studies [19]. The Crystal Vue is a novel 3D-US rendering technology that provided important sign and had a high clinical application value in some obstetric areas [18]. A multidimensional and intuitive diagnostic image can be produced by concurrently displaying the volume image and the perspective effect [17, 20]. Theophilus K. et al. had reported that 3D Volume Rendering US predicts the severity of PAS and involvement of the bladder [21]. The 3D Crystal Vue provided detailed information for the vesicouterine interfaces.

It is not necessary to perform an MRI to diagnose suspected PAS prenatally, but it has been suggested that MRI may have an advantage when it comes to detecting PP to parametrium and accessing posterior placenta, the invasion topography of PAS, and bladder invasion or obesity of pregnant women [14, 22–25]. A previous study [22] showed that MRI was highly specific (100%) in identifying bladder involvement (AUC=0.79,  $p=0.004$ ), with PPV equal to 100%. A prospective US and MRI comparative analysis [24] showed that loss of myometrial lining at the bladder interface on US, superior tenting of bladder wall, and bladder interface hypervascularity on color Doppler,

loss of chemical shift artifacts at the bladder–myometrial interface, was a sensitive and specific sign for detection of bladder involvement. The diagnostic accuracy of various US and MRI signs has also been reported [26, 27]. Extensive research on PAS from various countries reveals many close parallels; however, there are few articles on PAS disorder with bladder invasion.

Recent reports prove that the morbidity severity is dependent on the location of the PAS, the degree of neo-vascularization and involvement structure, and not necessarily the depth of villi invasion [28, 29]. In most cases, FIGO 1 do not require major surgery and can be managed conservatively [30]. Placenta increta or percreta, Often results in serious maternal morbidity and requires more invasive surgery, including hysterectomy [8, 9]. Therefore, the aim of prenatal imaging should be to detect PAS disorders of clinical significance such as placenta increta (FIGO 2) and percreta (FIGO 3). We collected the peripartum maternal and neonatal outcomes and screened the US and MRI signs of bladder involvement of PAS. This study aimed to evaluate the performance of 2D

US combined with 3D Crystal Vue and MRI in detecting bladder involvement in cases of PI and PP, and to help clinicians accurately assess a patient's condition and decide on a reasonable course of treatment.

## Materials and methods

### Patient information

In total, 111 pregnant women—whether or not they had placenta previa—between May 2019 and November 2023 at the First Affiliated Hospital of Anhui Medical University were included in the study if they were diagnosed of having PAS (PI or PP). Both US and MRI were used to evaluate 74 pregnant women. Total 53 pregnant women were ultimately included in our analysis (Fig. 1); the remaining 21 pregnant women were either lost to follow-up or image quality is poor. All of the pregnant women had cesarean sections. All of the clinical data was provided by the electronic case system.

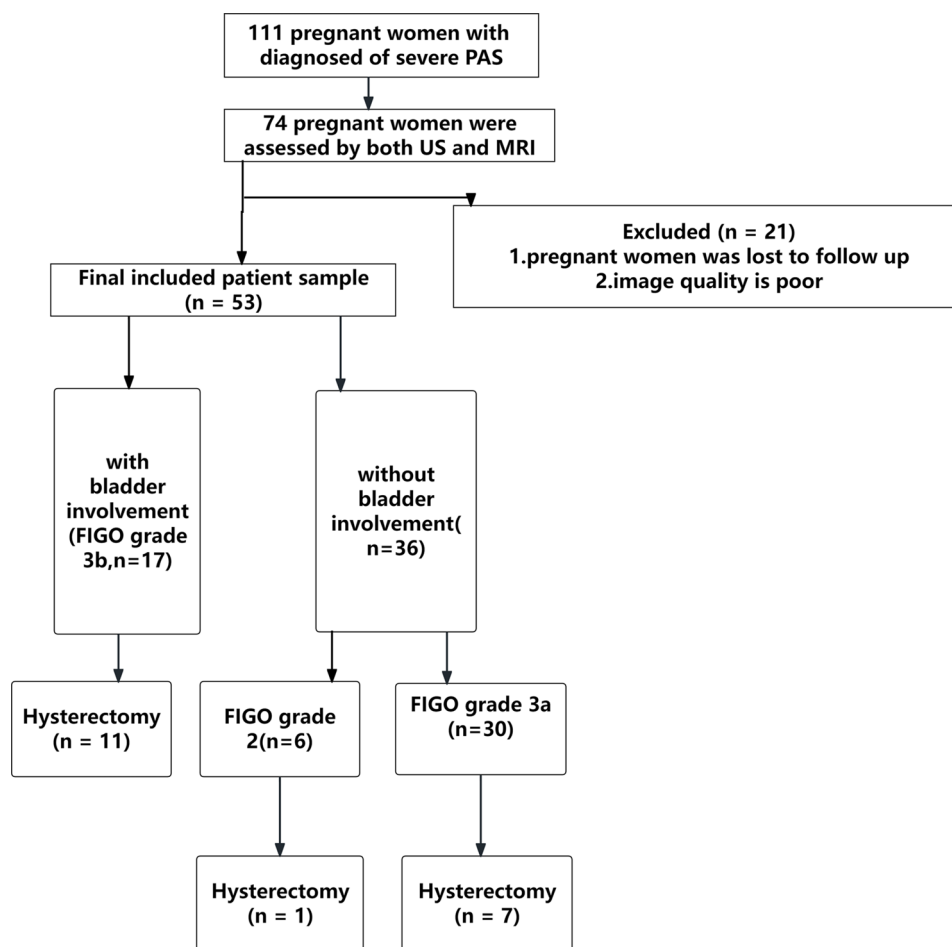


**Fig. 1** Flow chart shows inclusions and exclusions of the patients. US=ultrasound, FIGO=International Federation of Gynecology and Obstetrics, PAS=placenta accreta spectrum

### Instruments and equipment

#### **Prenatal US diagnosis of PAS was made by using a 1.0–8.0 MHz transabdominal, 2–9 MHz transabdominal and 3–10 MHz transvaginal transducer (Samsung HERAW10)**

To see uterine–bladder interface clearly, pregnant women should fill their bladders to the recommended capacity (200–300 cc). Both transvaginal and transabdominal US scans were performed on them. The PAS area was found in the 2D gray scale and color Doppler. The image features were recorded using the standardized US term proposed by the European Working Group on Abnormally Invasive Placentas (EW-AIP) and the AIP international expert group [31]. We also obtained additional 3D volumes from the sagittal section of the uterus, which we analysed by rotating a region of interest (ROI) so that it was perpendicular to the uterovesical interface. We collected and stored all 3D US volumes images for offline analysis. Then they switched to Render and used the “RealisticVue CrystalVue” modes. CrystalVue Present use 2 or 3. When the render direction is set to A +, rotate the X, Y, Z axes to obtain optimal information about the uterine bladder interface. At the same time, using the Crystal Vue to analyze with or without tramline’ sign showing the normal uterine–bladder interface [27, 32]. The “tramline sign” was identified as the presence of smooth contour hyper-echoic parallel lines representing the uterine serosa and bladder serosa and a sonolucent vesicouterine space in between [21]. It included three types: normal, “partially” obliterated, and “fully” obliterated (Fig. 2). “Partially” obliterated showed the disrupted the uterine serosa with a sonolucent vesicouterine space. “Fully” obliterated showed the disrupted bladder wall with obliterated vesicouterine space. Two physicians performed and independently reviewed the US without knowledge of the final clinical diagnosis (one with more than 15 years of experience, C.F.G., and the other with 10 years of experience, X.F.S. in obstetric scanning). The final diagnosis was reached through discussion and consultation if they disagreed.

#### **MRI imaging was performed using 3.0-T premier MRI (GE, Boston, MA, USA)**

T2 weighted single-short fast spin-echo (T2WI SSFSE) sequences were obtained using the following parameters: TR/TE, 1100/90; slice thickness, 4 mm; flip angle, 65°. The FIESTA sequences were acquired in three planes (axial, sagittal, and coronal) in all cases. T1 weighted gradient-echo imaging (T1WI) was conducted with a TR/TE of 112/2.0 ms, flip angle of 12°, and slice thickness of 4 mm. None of the pregnant patients in the study population received intravenous gadolinium contrast during MRI imaging, in accordance with the recommended imaging guidelines [33]. The radiologists (T.T.Z. and H.W.L. had ten years of MRI experience) independently reviewed MRI images without knowledge of the final diagnosis. If the two radiologists could not agree on a final diagnosis, a consultation was conducted. MRI images were analyzed and recorded using the Unified and Standardized MRI Descriptors developed by the International Society for AIP [34]. In addition, the “bladder vessel” sign and bladder tenting were recorded. The “bladder vessel” sign is characterized by an extensive flow void network extending from the uterine serosa to the vesicouterine space, with markedly increased vascularity observed at the interface between the uterus and bladder (Fig. 3). Bladder tenting refers to elevation of the bladder dome toward the uterine surface.

#### **Standards of reference**

The diagnostic standard was determined using clinical and histological criteria according to the International Federation of Gynecology and Obstetrics (FIGO) classification for PAS [3]. Our diagnoses of bladder invasion (Grade 3b) are either of the following.

#### **Clinical standards**

No other organs are visible, but the placental villi occupying the bladder make it impossible to identify the surgical uterine–bladder plane.

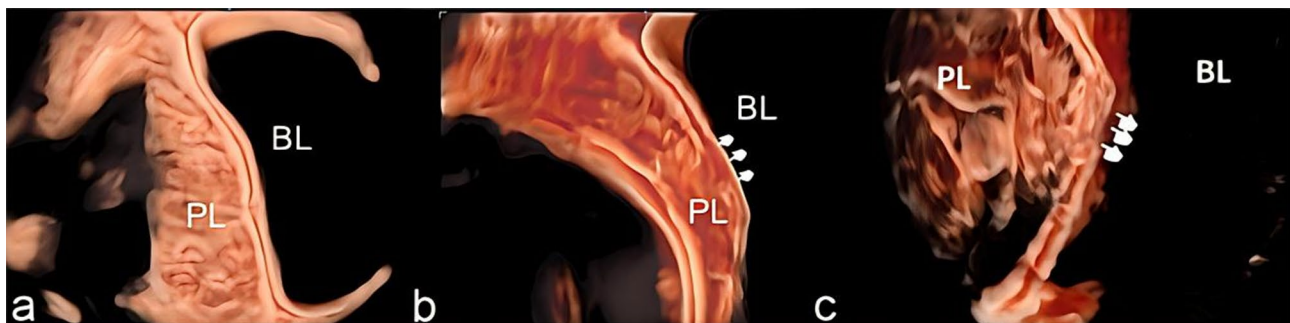


**Fig. 2** a. A normal uterine-serosal and uterine-bladder interface was observed; b. “partially” obliterated interfaces, displaying the destruction of the uterine-serosal interface; c. “fully” obliterated, indicating disruption of both the uterine-bladder interfaces (arrows)

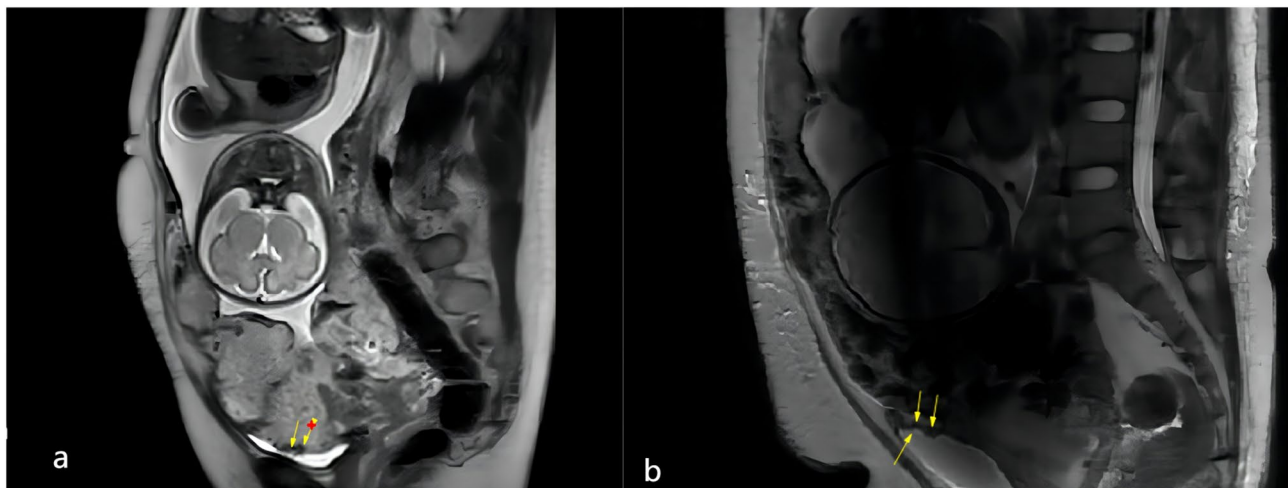


**Fig. 3** a. Abnormal vascularization of the placental bed (arrows) b. Focal exophytic mass (arrows)

**Table 1** Comparison of the basic data and related pregnancy history of the two groups

Characteristic	No bladder involvement (N=36)	bladder Involvement (N=17)	P
Age (y)	34.7 ± 4.2	35.9 ± 4.7	0.355
GA at delivery, wk	35(34.0,36.0)	35(34.5,37.5)	0.390
M(P25,P75)	33.98–36.02	33.88–37.29	
95% CI			
Height, cm	160.3 ± 5.3	160.8 ± 3.5	0.702
Weight, kg	69.2 ± 7.9	69.1 ± 1.5	0.975
Placenta position			0.387
Normal	5	2	
low-lying placenta	3	4	
Placenta previa	28	11	
ART	6(16.67%)	3(17.6%)	1.000
Previous uterine surgery			0.830
0	20(55.56%)	11(64.71%)	
1	12(33.33%)	5(29.41%)	
≥ 2	4(11.11%)	1(5.88%)	
No. of previous CS			0.915
0	5	2	
1	21	9	
≥ 2	10	6	
CSP	6(16.7%)	15(88.25%)	<b>0.000</b>
FIGO grade of PAS			NA
2	6(16.67%)	0	
3a	30(83.33%)	0	
3b	0	17(100%)	
3c	0	0	
No. of previous PAS			<b>0.004</b>
0	34(94.44%)	12(70.59%)	
1	2(5.56%)	5(29.41%)	
≥ 2	0	0	

GA: gestational age, CS: cesarean section, CSP: Cesarean scar pregnancy, ART: assisted reproductive technique, CI: confidence intervals, PAS: placenta accreta spectrum

### Histologic standards

An example of villous tissue penetrating the bladder wall from a hysterectomy specimen.

### Statistical analysis

The data were analyzed using Meta-DiSc and SPSS (version 17.0). For continuous variables with a normal distribution, data are presented as mean ± standard deviation (SD), and the t-test can be used to find the p-value between groups. For variables with a skewed distribution, the expression is P25, P75, and the Mann–Whitney U test can be used to find the p-value. For categorical variables, the  $\chi^2$  test or Fisher's exact probability test were used to compare differences between groups. The statistical software package Meta-Disc was used to analyze the accuracy, sensitivity, specificity, positive predictive value (PPV) and negative predictive value (NPV) of the US and MRI findings. 95% confidence intervals (CI) was used to express indicator and effect values. Multivariate and univariate logistic regressions were used to explore the diagnostic efficiencies of US and MRI. Delong test was used to compare AUC values.  $P < 0.05$  was deemed statistically significant.

### Results

#### Baseline data

The demographic features and surgical PAS outcomes of the cases are compared in Table 1. It was observed that 5 of 17 (29.41%) patients with bladder involvement had a history of PAS and 2 of 36(5.56%) patients without bladder involvement had a history of PAS in previous pregnancies ( $p < 0.01$ ). There were no statistically significant variations in other basic statistics between the groups, however, patients with bladder involvement had a greater rate of cesarean scar pregnancy ( $p < 0.01$ ) than patients without bladder involvement.

### Maternal and neonatal outcomes

Table 2 presents a comparison of the maternal and newborn outcomes of patients with PAS. First, patients with bladder involvement had a greater rate of hysterectomy than patients without bladder involvement ( $p < 0.01$ ). Secondly, patients with bladder involvement spent more days in the hospital after surgery than patients without bladder involvement ( $p < 0.01$ ). Furthermore, compared to patients without bladder involvement, patients with bladder involvement required more ICU stays ( $p = 0.019$ ). PAS patients with bladder involvement were more likely to require ureteroscopy or cystoscopy ( $p < 0.01$ ). Concurrently, individuals with bladder involvement exhibited a higher likelihood of necessitating embolization of the internal iliac arteries and uterine artery embolization ( $p < 0.01$ ). There was no discernible difference in the groups' perioperative blood transfusion needs, estimated blood loss, fetal weight, or 5-min APGAR score  $< 7$  ( $P > 0.05$ ).

### US and MRI diagnostic performance for PAS with bladder involvement

#### The US study's findings are reported in table 3

In terms of US findings, there was no significant difference between the two groups regarding the frequency of Loss of "clear zone", Placental lacunae, Myometrial Thinning, and Subplacental Hypervascularity ( $p > 0.05$ ). Of the ten US findings, the tramline sign "fully" obliterated on 3D Crystal Vue had the highest accuracy (92.45%, 95%CI, 81.79–91.91). Patients with PAS and bladder involvement tended to occur more frequently (all  $p \leq 0.05$ ) of bridging vessels, placental bulge, bladder wall interruption, uterovesical hypervascularity, focal exophytic mass, and the tramline sign "fully" obliterated on 3D Crystal Vue. Bladder wall interruption had

the highest accuracy among the 2D US signs, measuring 83.02% (95%CI, 70.20–91.93), it was followed by focal exophytic mass (77.35%) and placental bulge (75.47%). Of these, focal exophytic mass showed the highest specificity (100%, 95%CI, 90.26–100) and the lowest sensitivities (29.41%, 95%CI, 10.31–55.96), while Bladder wall interruption showed the highest sensitivity (100%, 95%CI, 80.49–100), followed by uterovesical hypervascularity (94.12%, 95%CI, 71.31–99.85) and the tramline sign "fully" obliterated (88.23%, 95%CI, 63.56–98.54). The tramline sign "fully" obliterated on Crystal Vue had the highest diagnostic accuracy (AUC of 0.91, 95%CI, 0.75–1.0), followed by bladder wall interruption (AUC of 0.88, 95%CI, 0.78–0.97) for identifying bladder involvement in patients with severe PAS diseases (Table 3). The US feature ROC curves for bladder involvement diagnosis are displayed in (Fig. 4).

#### Table 3 presents an overview of the MRI study's findings

On MRI, the bladder-involved patients of severe PAS, compared with bladder-uninvolved patients, showed a higher frequency (all  $p \leq 0.05$ ) of Placental bulge, bladder wall interruption, bladder tenting, focal exophytic mass, bladder vessel sign. None of the findings (myometrial thinning, dark intraplacental bands, loss of retroplacental dark zone, heterogeneous placenta, abnormal vascularization of the placental bed) between the two groups showed a statistically significant difference ( $p > 0.05$ ). Among the ten MRI findings, accuracy was highest for bladder tenting (75.47%), bladder wall interruption (75.47%), bladder vessel sign (75.47%), and placental bulge (75.47%, 95%CI, 26.45–54.00), followed by focal exophytic mass (73.58%, 95%CI, 63.79–87.72). The focal exophytic mass, bladder tenting, and bladder wall interruption had high specificity (94.44%, 88.89%, and 77.78%,

**Table 2** Characteristics of maternal and neonatal outcomes

Variable	No bladder involvement (N = 36)	bladder Involvement (N = 17)	Pvalue
Blood transfusion	25(69.44%)	14(82.35%)	0.508
Estimated blood loss (mL)	1850.00(1000.00, 2500.00)	1500.00(750.00, 2250.00)	0.559
M(P25,P75)	(1514.49-2413.28)	1138.88–2367.00	
95% CI			
Number of days in hospital postoperative(d)	9.0(6.00, 11.75)	11.0(8.00, 19.00)	<b>0.039</b>
M(P25,P75)	8.35–12.43	10.16–17.49	
95% CI			
fetal weight(g)	2672.1 ± 440.8	2720.6 ± 872.3	0.789
ICU	11(30.56%)	11(64.70%)	<b>0.019</b>
5-min APGAR score < 7	1(2.78%)	2(11.76%)	0.238
Hysterectomy	8(22.22%)	11(64.71%)	<b>0.003</b>
Cystoscopy or Ureteroscopy	3(8.33%)	16(94.12%)	<b>0.000</b>
Uterine artery embolization	4(11.11%)	8(47.06%)	<b>0.001</b>
Embolization of the internal iliac arteries	2(5.56%)	5(29.41%)	<b>0.004</b>

ICU: intensive care unit

**Table 3** Analysis of US and MRI signs in the detection of bladder involvement

US	No bladder involvement (N=36)	bladder involvement (N=17)	Accuracy (%)	Sensitivity(%)	Specificity(%)	PPV(%)	NPV(%)	P	AUC
Loss of "clear zone" 95% CI	34(94.44%)	17(100%)	35.85 23.14–50.20	100 80.49–100.00	5.56 0.68–18.66	33.33 20.76–47.92	100 15.81–100.00	1.000	0.53 0.36–0.69
Placental lacunae 95% CI	30(83.33%)	14(82.35%)	37.73 24.79–50.11	82.35 56.57–96.20	16.67 6.37–32.81	31.82 18.61–47.58	66.67 29.93–92.51	1.000	0.50 0.33–0.66
Myometrial thinning 95% CI	33(91.67%)	17(100%)	37.73 24.79–52.11	100.00 80.49–100.00	8.33 1.75–22.47	34.00 21.21–48.77	100 29.24–100.00	0.543	0.54 0.38–0.71
Subplacental hypervascularity 95% CI	28(77.78%)	13(76.47%)	39.62 26.45–54.00	76.47 50.10–93.19	22.22 10.12–39.15	31.71 25.28–38.91	66.67 41.11–85.14	1.000	0.49 0.33–0.66
Bridging vessels 95% CI	18(50%)	16(94.11%)	64.15 49.80–76.86	94.12 71.31–99.85	50.00 32.92–67.08	47.06 29.78–64.87	94.74 73.97–99.87	0.002	0.72 0.58–0.86
Placental bulge 95% CI	4(11.11%)	8(47.06%)	75.47 61.72–86.24	47.06 22.98–72.19	88.89 73.94–96.89	66.67 41.11–85.14	78.05 69.05–84.96	0.001	0.68 0.51–0.84
Bladder wall interruption 95% CI	9(25%)	17(100%)	83.02 70.20–91.93	100.00 80.49–100	75.00 57.80–87.88	65.38 44.33–82.79	100 87.23–100.00	0.000	0.88 0.78–0.97
Uterovesical hypervascularity 95% CI	21(58.33%)	16(94.12%)	58.49 44.13–71.86	94.12 71.31–99.85	41.67 25.51–59.24	43.24 27.10–60.51	93.75 69.77–99.84	0.008	0.68 0.53–0.82
Focal exophytic mass 95% CI	0	5(29.41%)	77.35 63.79–87.72	29.41 10.31–55.96	100 90.26–100.00	100	75.00 68.82–80.30	0.004	0.65 0.50–0.77
The tramline sign "fully" obliterated on 3D Crystal Vue 95% CI	2(5.56%)	15(88.23%)	92.45 81.79–97.91	88.23 63.56–98.54	94.44 81.34–99.32	88.23 65.85–96.68	94.44 82.19–98.43	0.000	0.913 0.75–1.00
MRI	No bladder involvement (N=36)	bladder involvement (N=17)	Accuracy	Sensitivity(%)	Specificity(%)	PPV(%)	NPV(%)	P	AUC
Myometrial thinning 95% CI	31(86.11%)	16(94.11%)	39.62 26.45–54.00	94.12 71.33–99.85	13.89 4.67–29.50	34.04 30.19–38.12	83.33 38.73–97.53	0.693	0.54 0.38–0.70
Dark intraplacental bands 95% CI	32(88.89%)	15(88.23%)	35.85 23.14–50.20	88.23 63.56–98.54	11.11 3.11–26.06	31.92 27.56–36.61	66.67 28.84–90.80	1.000	0.50 0.33–0.67
Placental bulge 95% CI	12(33.33%)	16(94.12%)	75.47 61.72–86.24	94.12 71.31–99.85	66.67 49.03–81.44	57.14 45.28–68.24	96.00 77.95–99.39	0.000	0.80 0.68–0.92
Loss of retroplacental dark zone 95% CI	31(86.11%)	16(94.12%)	39.62 26.45–54.00	94.12 71.31–99.85	13.89 4.67–29.50	34.04 30.19–38.12	83.33 38.73–97.53	0.693	0.54 0.38–0.70
Bladder wall interruption 95% CI	8(22.22%)	12(70.59%)	75.47 61.72–86.24	70.59 44.04–89.69	77.78 60.85–89.89	60.00 43.09–74.83	84.85 72.43–92.27	0.001	0.74 0.59–0.89
Focal exophytic mass 95% CI	2(5.56%)	5(29.41%)	73.58 63.79–87.72	29.41 10.31–55.96	94.44 81.34–99.32	71.43 35.00–92.06	73.91 67.36–79.55	0.004	0.62 0.48–0.75
Heterogeneous placenta 95% CI	31(86.11%)	16(94.12%)	39.62 26.45–54.00	94.12 71.31–99.85	13.89 4.67–29.50	34.04 30.19–38.12	83.33 38.73–97.53	0.693	0.54 0.38–0.70
Abnormal vascularization of the placental bed 95% CI	24(66.67%)	13(76.47%)	47.17 33.30–61.36	76.47 50.10–93.19	33.33 18.56–50.97	35.13 27.62–43.47	75.00 53.12–88.82	0.468	0.55 0.38–0.71

**Table 3** (continued)

US	No bladder involvement (N=36)	bladder involvement (N=17)	Accuracy (%)	Sensitivity(%)	Specificity(%)	PPV(%)	NPV(%)	P	AUC
Bladder tenting	4(11.11%)	8(47.06%)	75.47	47.06	88.89	66.67	78.05	0.001	0.68
95% CI			61.72–86.24	22.98–72.19	73.94–96.89	41.11–85.14	69.05–84.96		0.51–0.84
Bladder vessel sign	9(25%)	13(76.47%)	75.47	76.47	75.00	59.09	87.10	0.001	0.76
95% CI			61.72–86.24	50.10–93.19	57.80–87.88	43.62–72.95	73.73–94.20		0.61–0.90

CI: confidence intervals

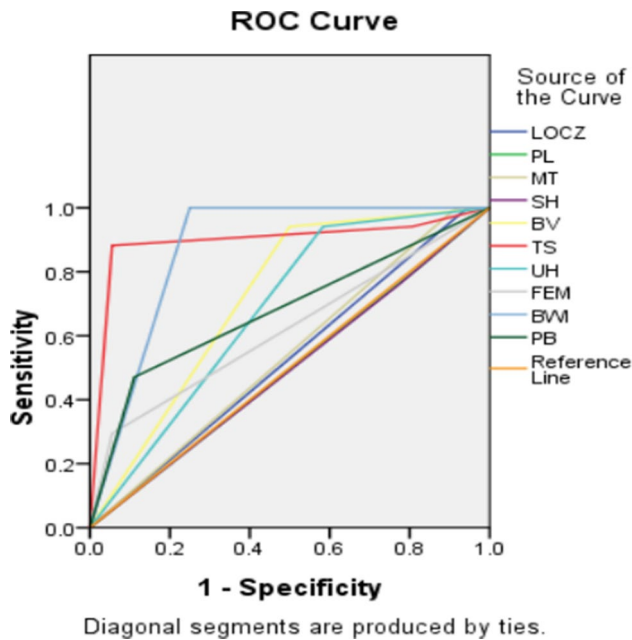


**Fig. 4** ROC curves of the use of US features for diagnosing bladder involvement in severe PAS disorders. LOCZ: Loss of “clear zone”, PL: placental lacunae, MT: Myometrial thinning, SH: Subplacental hypervascularity, BV: Bridging vessels, PB: Placental bulge, BWI: Bladder wall interruption, UH: Uterovesical hypervascularity, FEM: Focal exophytic mass, TS: the tramline sign “fully” obliterated on 3D Crystal Vue

respectively) but low sensitivity (29.41%, 47.06%, 70.59%, respectively). The MRI finding with the highest sensitivity of 94.12%, 95% CI, 71.31–99.85) was myometrial thinning, loss of retroplacental dark zone, placental bulge, and heterogeneous placenta. For detecting bladder involvement of patients with severe PAS, the placental bulge achieved the highest diagnostic accuracy with an AUC of 0.80 (95% CI, 0.68–0.92), followed by the bladder vessel sign feature with AUC of 0.76 (95% CI, 0.61–0.9) (Table 3). The ROC curves of MRI features for diagnosis of bladder involvement are shown in Fig. 5.

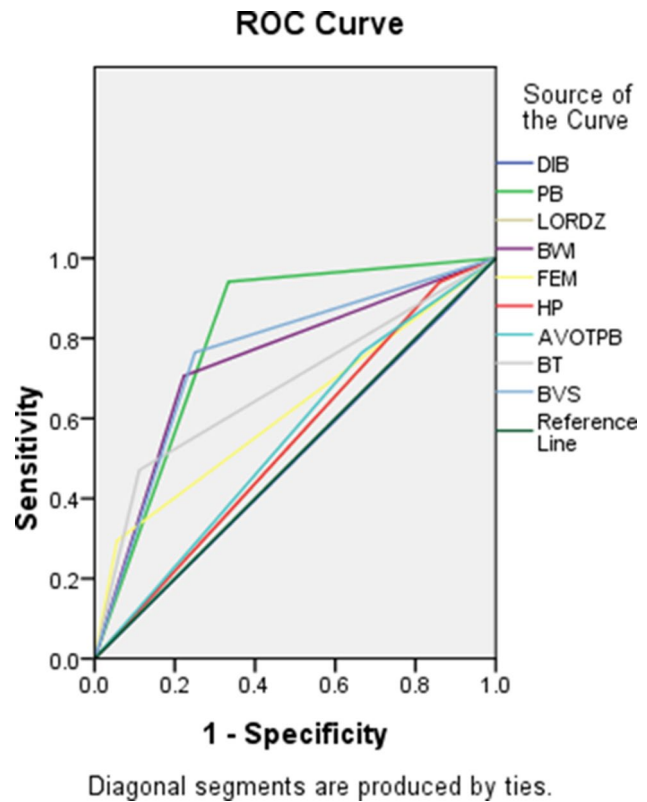


**Fig. 5** ROC curves of the use of MRI features for diagnosing bladder involvement in severe PAS disorders. BI: bladder involvement, MT: Myometrial thinning, DIB: Dark intraplacental bands, Placental bulge, LORDZ: Loss of retroplacental dark zone, BWI: Bladder wall interruption, FEM: Focal exophytic mass, HP: Heterogeneous placenta, AVOTPB: Abnormal vascularization of the placental bed, BT: bladder tenting, BVS: bladder vessel sign

**AUC curve and multivariable logistic regression analysis**

**Multiple variable logistic regression analysis of US features to forecast pas disorders’ bladder involvement**

The study employed multivariate logistic regression analysis to identify independent predictive features in patients with bladder invasion (Table 4). Three US findings (Bridging vessels, Uterovesical hypervascularity, The tramline sign “fully” obliterated on Crystal Vue) were entered into the multivariable logistic regression analysis for predicting bladder invasion. Multiple logistic regression analysis found that the bridging vessels



**Table 4** Significant US and MRI features for predicting bladder involvement in severe PAS, determined by univariate and multivariate logistic regression analyses

US Variable	Univariate		Multivariate		MRI Variable	Univariate		Multivariate	
	OR (95% CI)	p	OR (95% CI)	p		OR (95% CI)	p	OR (95% CI)	p
Loss of "clear zone"	NA	0.999	NA	NA	Myometrial thinning	2.581 (0.277–24.004)	0.405	NA	NA
Placental lacunae	0.933 (0.203–4.285)	0.929	NA	NA	Dark intraplacental bands	0.938 (0.154–5.699)	0.944	NA	NA
Myometrial thinning	NA	0.999	NA	NA	Placental bulge	32.00 (3.781–270.848)	<b>0.001</b>	57.00 (3.89–835.80)	<b>0.003</b>
Subplacental hypervascularity	0.929 (0.236–3.649)	0.915	NA	NA	Loss of retroplacental dark zone	2.581 (0.277–24.004)	0.405	NA	NA
Bridging vessels	16.000 (1.914–33.738)	<b>0.010</b>	31.76	<b>0.010</b>	Bladder wall interruption	8.4 (2.275–31.009)	<b>0.001</b>	11.93 (1.60–88.85)	<b>0.016</b>
Placental bulge	176.000 (1.943–1828.208)	0.294	NA	NA	Focal exophytic mass	7.08 (1.21–41.459)	<b>0.030</b>	NA	NA
Bladder wall interruption	NA	0.998	NA	NA	Heterogeneous placenta	2.581 (0.277–24.004)	0.405	NA	NA
Uterovesical hypervascularity	11.429 (1.363–95.802)	<b>0.025</b>	NA	NA	Abnormal vascularization of the placental bed	1.625 (0.435–6.068)	0.470	NA	NA
Focal exophytic mass	NA	0.999	NA	NA	Bladder tenting	7.111 (1.737–29.120)	<b>0.006</b>	NA	NA
The tramline sign "fully" obliterated on 3D Crystal Vue	39.963 (7.275–219.520)	<b>0.000</b>	68.92 (6.76–702.35)	<b>0.000</b>	Bladder vessel sign	5.75 (1.550–21.329)	<b>0.009</b>	9.75 (1.43–66.21)	<b>0.020</b>

NA = not applicable, CI: confidence intervals, OR: odds Ratio

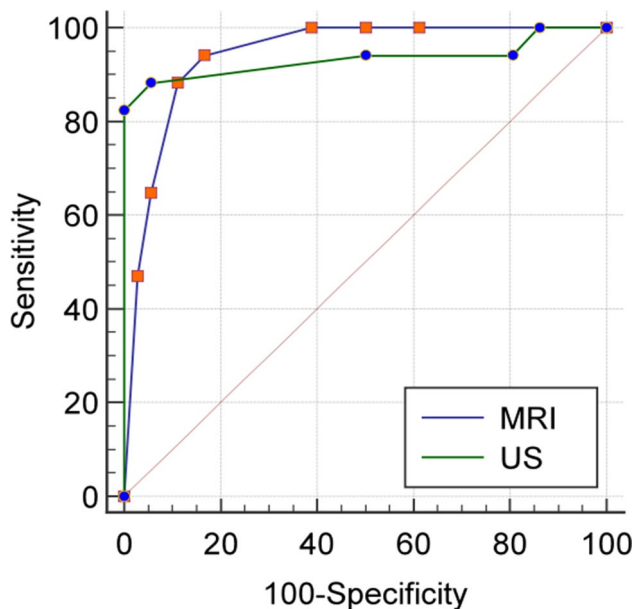


**Fig. 6** ROC analysis of combined US and MRI features to calculate the AUC for detecting bladder involvement in severe PAS disorders

(OR, 31.76, 95% CI, 1.64–614.31,  $p=0.022$ ) and the tramline sign "fully" obliterated on Crystal Vue feature (OR, 68.92; 95% CI, 6.76–702.35,  $p<0.001$ ) were independently associated with an increased likelihood of bladder involvement. These findings when combined allowed

for the prediction of bladder involvement with an 88.2% sensitivity, a 94.4% specificity, and an AUC of 0.933 (95% CI, 0.829–0.983,  $p=0.001$ ). Figure 6 displays the integrated risk prediction model and ROC curve of our risk factor.

**Multivariable logistic regression analysis of MRI features to predict pas disorders associated with the bladder involvement**

Five MRI signs (Placental bulge, Focal exophytic mass, Bladder tenting, Bladder wall interruption, Bladder vessel sign) were entered into the multivariable logistic regression analysis for predicting bladder involvement. The results of the logistic regression analysis were as follows: the three independent risk factors for bladder involvement were: Placental bulge (OR, 57.99, 95% CI, 3.89–835.80,  $p=0.003$ ), Bladder wall interruption (OR, 11.93, 95% CI, 1.60–88.85,  $p=0.016$ ), and Bladder vessel sign (OR, 9.75, 95% CI, 1.43–66.21,  $p=0.020$ ) (Table 4). The joint diagnosis of these three risk factors showed a sensitivity of 94.1% and specificity of 83.3%. The area under the curve was 0.942 (95% CI, 0.841–0.988,  $p<0.001$ ). The risk prediction model and ROC curve of MRI risk factor are displayed in Fig. 6.

There is no statistically significant difference between the two prediction models' area under the ROC curves ( $P=0.876$ , 95% CI, -0.104–0.122).

## Discussion

Severe postpartum hemorrhage (SPPH) is a major cause of maternal death and severe maternal morbidity. Placenta previa (aOR=9.75, 95% CI: 7.45–12.75) and PAS (aOR=8.00, 95% CI: 6.20–10.33) are significant risk factors for Severe postpartum hemorrhage (SPPH) [35]. In many countries, placenta accreta spectrum disorders are on the rise. The high cesarean rates acted as a catalyst for PAS incidence [36]. The previous study identified two potential factors when it came to the risks of PAS: one had a previous cesarean delivery, and the other had a previa placenta [37]. Cesarean scar pregnancy is a known trigger for PAS disorders [1]. In the present study, we found that the rate of cesarean scar pregnancy was higher in patients with bladder involvement than in those without bladder involvement ( $p < 0.01$ ). A study based on 10 cases of cesarean scar pregnancy (CSP) showed that CSP is a precursor of PAS, both sharing the same histopathology [38]. Thus, this early detection of CSP is crucial. In our study, 5 of 17 (29.41%) patients with bladder invasion had a history of PAS in previous pregnancies. Aligns with Bhatia et al. [39] study, women with CS who underwent placental implantation over a lower uterine scar had an increased risk of developing PAS problems.

In certain cases of PP, a large number of newly developed vessels may impede bladder dissection and result in excessive bleeding [40]. Numerous problems, including an elevated risk of bleeding during and after pregnancy, the need for blood transfusions, sepsis, hysterectomy, and the need to move the mother to urgent care, can result from PAS. Additionally, prematurity, low Apgar scores, and neonatal and fetal death are linked to PAS. Bladder involvement in PP is an uncommon but dangerous condition. Ureteric stent placement before surgery is especially advised to minimize urinary tract damage [41]. A ureteric stent can be implanted during a cystoscopy or ureteroscopy to address bladder invasion caused by the placenta. Surgeon preference is responsible for the inconsistent usage of cystoscopy or ureteroscopy [41]. A complete or partial hysterectomy was performed in almost all PP instances including bladder involvement [42]. In this study, 11 patients who had bladder involvement underwent a hysterectomy; these patients also had a greater rate of ureteric stent use and hysterectomy overall. Prophylactic abdominal aortic balloon occlusion (AABO), uterine arterial embolization, iliac internal artery ligation (IIAL), and uterine artery ligation (UAL) are some of the procedures certain institutions [22, 40, 43, 44] may use to reduce hemorrhage operation complications. A retrospective case control study showed that an internal iliac artery balloon placement did not reduce the amount of intraoperative bleeding or the need for hysterectomy [45]. It is important to balance the benefits of reducing blood loss with the risks of adverse maternal outcomes

include vascular injury and thrombus formation. During hysterectomy, neither balloon placement nor intraoperative ligation is supported by the current evidence [9]. Reported strategies for Bladder invasion include obstetric hysterectomy, leaving the placenta in situ with postoperative methotrexate therapy and removal of the placenta with bladder reconstruction in a single stage [13]. Optimizing diagnosis and treatment can lead to better postnatal outcomes, especially when the PAS is carried out by a general hospital or by a skilled operator [16, 44, 46, 47]. Definitive preoperative diagnosis helps to fully prepare and organize multidisciplinary (a team of physicians and surgeons representing urology, radiology, and obstetrics-gynecology) assistance for complex surgery that may require massive blood transfusion [48].

In our study, out of the ten US findings, accuracy was highest for the tramline sign “fully” obliterated on 3D Crystal Vue (92.45%). The tramline sign “fully” obliterated showed high specificity (94.44%) and high sensitivities (88.23%). More detail, including solid and distinct soft tissue outlines, is possible because of 3D. The bladder mucosa and uterine serosa are represented by the “tramline” sign [21, 27, 32]. According to a recent study, “partially or fully obliterated” tramline signs on 3D Crystal Vue have a strong association with indications of operative complexity, postnatal confirmation of PAS, and peripartum hysterectomy [27]. According to Shaoqi Chen et al., a 2D ultrasound overdiagnosis was reversed by Crystal Vue. The 2D US showed an uneven bladder wall and worrisome bladder involvement, but the whole tramline was visible in the Crystal Vue image, indicating that the placenta was correctly identified as PA rather than PP. As a supplementary method, 3D US can be used to diagnose or rule out PP [19]. On 3D Crystal Vue, the tramline sign “fully” obliterated had great AUC of 0.913 ( $p = 0.000$ , CI 0.75–1.00) to predict bladder invasion. This finding is consistent with that of Theophilus K. et al. who showed that all the US signs, the 3D disrupted urinary bladder wall with obliterated vesicouterine space was the only predictor for bladder involvement with an OR of 27 (95% CI 3.8–191.7,  $p < 0.001$ ) [21]. A “rail sign” is defined as two parallel neovascularizations over the bladder mucosa and uterovesical junction that are joined by bridge vessels that are perpendicular to both [49]. Rail symptoms were identified as an independent risk factor for bladder invasion in their sample (OR, 3.86; 95% CI, 1.04–14.41;  $P = 0.033$ ). If a rail sign is negative, the NPV of bladder invasion is 95.1%, indicating high confidence in rejecting bladder invasion. Despite the fact that “rail sign” and “tramline” sign are similar terms, researchers must acknowledge that their clinical implications are different. In our study, according to multiple logistic regression analysis, bridging vessels (OR, 31.76, 95% CI: 1.64–614.31,  $p = 0.022$ ) and the tramline sign “fully” obliterated on 3D Crystal Vue

(OR, 68.92, 95%CI, 6.76–702.35,  $p < 0.001$ ) were linked to the existence of bladder involvement. The combined results had an 88.2% sensitivity, a 94.4% specificity, and an AUC of 0.933 ( $p = 0.001$ ). Bridging vessels illustrates the presence of serosal neovascularity which could be sometimes seen to have vascular anastomosis with the vesical vessels [50, 51]. Rather than traverse the myometrium and bladder, these vessels are actually the contorted vessels of the neovascularity within the serosal. Even though in our study bridging vessels could be seen in almost case of bladder involvement, in clinical practice, the presence of bridging vessels could be seen with or without bladder involvement. There are probably still too few cases studied. 2D US signs accuracy was highest for Bladder wall interruption (83.02%), showed high sensitivity (100%) and a 75% specificity. The disruption of the bladder wall in 2D grayscale could indicate that the placental villi had invaded the bladder wall [31], but bladder wall interruption also indicates serosal neovascularity and is most likely an ultrasound artefact arising from the massive neovascularization [1, 50] or Urinary bladder varices [52]. It is very difficult to identify on the 2D US. Our study included a case in which a 2D gray and CDFI ultrasound revealed an interrupted bladder wall and uterovesical hypervascularity, raising suspicion of bladder implantation. However, 3D crystal imaging indicated that the vessel was highlighting the uterine wall rather than interruption of the bladder wall, with postoperative findings confirming placental implantation.

The study's data [53] showed that the subjective appearance of hypervascularity, myometrial thickness, bladder wall interruption, and placental bulge, as well as the US and MRI markers of PAS abnormalities, change as the bladder fills. When the bladder is empty, it is challenging to identify placental bulging into the surrounding tissue. Furthermore, a decrease of myometrium thickness and the retroplacental clear zone may arise from high probe pressure [30]. A prior study [54] found that in the multivariable regression analysis, placental bulge was an independent predictor of severe PAS on US (OR, 8.94;  $p = 0.02$ ) and MRI (OR, 45.67;  $p = 0.003$ ). The results of our investigation indicated that the placental bulge had a high specificity of 88.89%, accuracy of 75.47%, lower sensitivity of 47.06%, and an AUC of 0.68 (CI, 0.51–0.8,  $p = 0.001$ ) on US and an AUC of 0.80 (CI, 0.68–0.92,  $p = 0.000$ ) on MRI. This aligns with the findings of earlier research [55]. Researchers frequently employ subjective descriptions of symptoms; therefore, several labels may be applied to the same condition. The placental bed's abnormal vascularization, the uterovesical interface's abnormal vascularization, the bladder vessel sign, and the serosal vessel sign are all indicators of abnormal vascularization. While not exact replicas, these signs are similar. They stand for various vascularization intensities. They might be involved

in the same pathological mechanism. 2D color Numerous parameters, including patient fat and thinness, bladder capacity, operator manipulation, and instrument settings, influence the Doppler blood flow display. Compared to grey-scale imaging, operator error is more likely to occur with CDFI. According to an observational case-control research, sonography can be used as an additional marker to identify pulsing veins at the posterior bladder wall with a low RI early in pregnancy, which can help diagnosis severe PAS disease [56]. To validate this quantitative report—which is still comparatively uncommon—many more investigations are required.

The detection of invasive placental diseases can be accomplished with both MRI and US, according to a prospective US and MRI comparison investigation [24]. MRI, however, provides a more accurate prediction of bladder invasion. When MR and US were compared for the diagnosis of placental adhesive problems, Masselli et al. [57] discovered that MRI was a very useful method for topographic assessment and staging of these illnesses ( $P < 0.001$ ). Excellent indicators of the extent and intensity of placental invasion are provided by placental MRI [58]. MRI was performed on a subset of the ultrasonography-screened group in multiple trials. We must acknowledge that, in cases when a hysterectomy is planned or the placenta is placed in the posterior wall, MRI should be the method of choice for determining the topography and depth of placental invasion [23]. According to our research, bladder invasion might be independently predicted by MRI indicators for placental bulge, bladder wall interruption, and bladder vessel sign. The results of the logistic regression analysis indicated that bladder wall interruption (OR, 11.93; 95%CI, 1.60–88.85,  $p = 0.016$ ), bladder vessel sign (OR, 9.75; 95%CI, 1.43–66.21;  $p = 0.020$ ), and placental bulge (OR, 57.99; 95%CI, 3.89–835.80,  $p = 0.003$ ) were independent risk variables of severe PAS of bladder involvement. The combined diagnosis had an 83.5% specificity and 94.1% sensitivity. 0.942 was the area under the curve (95%CI, 0.841–0.988,  $p < 0.001$ ). A Prospective Evaluation [22] reported Bladder vessel sign (OR, 5.73; 95% CI, 1.14–28.79;  $p = 0.021$ ) and serosal vessel sign (OR, 14.72; 95% CI, 2.82–76.83;  $p = 0.001$ ) were found to be independent predictors of bladder involvement by multiple logistic regression analysis [22]. Bladder vessel sign was by far the most accurate predictor for bladder involvement (AUC = 0.96,  $p < 0.001$ ) with sensitivity, specificity, PPV, and NPV of greater than 95% [22]. Consistent with the previous literature [14, 22], Bladder tenting was another significant predictor but an only moderately accurate (AUC = 0.68,  $p < 0.001$ ) figures for bladder invasion in PAS. A explanation for this result change as the bladder fills. A focal exophytic mass on MRI can raise the concern of bladder invasion, but lower

sensitivity(29.41%,95%CI,10.31–55.96),this finding is consistent with the previous literature [14].It seems possible that the rarity of the sign.According to Watchaya Jariyawattanarat et al. [14], abnormal vascularization at the uterovesical interface on MRI and the absence of chemical shift artifacts in the steady-state free precession sequence together predicted bladder involvement with high specificity, demonstrating the highest specificity and PPV of 100%, a sensitivity of 38%, and an NPV of 66% ( $p < 0.001$ ).

It is important to acknowledge that not every PAS patient with bladder involvement will exhibit all aberrant indications, and that not every sign will imply bladder implantation. This also explains why there is no gold standard for indicators of bladder involvement in any of the signs.

### Strengths and limitations

Although many articles have evaluated the value of ultrasound and MR in the diagnosis of placenta implantation, few articles have compared the value of both in bladder implantation.We did not compare 2 D US with MRI; instead, we compared 2D integrated 3D Crystal Vue with MRI. We examined the accuracy, sensitivity, specificity, and other aspects of each sign due to other clinical and pathological variables associated with each symptom. Since subjective factors can easily influence sticky placenta implantation, a definitive diagnosis is difficult to achieve. Patients with PI and PP are the study's target population because they are clinically and pathologically complex and challenging to diagnose.

### Limitations

First, this was a retrospective study. Secondly, the sample size in this study was somewhat small, However, this number allowed an adequate statistical analysis.The incident of bladder invasion was low. Compare with other institutions, there are still a lot of patients with bladder involvement overall.Because we are a complete hospital, many pregnant women are referred from small hospitals to our hospital. Furthermore, it's possible that the doctors' selection and the referral cases overstated the precision of the two methods. Afterall, All of our physicians are attending physicians and senior associate chief physicians.The referral cases adds some detail and improves the accuracy of our assessment. We believed experienced and skilled physicians are needed and severe PAS patients showed also be transferred to a specialist hospital. Because MRIs are only performed in our hospital when PAS is suspected, evaluating their performance is skewed. As a result, it also somewhat increases diagnostic accuracy.Multicenter approach should be used in future studies to create more dependable models.

### Conclusions

Both 2D coupled 3D Crystal Vue imaging and MRI are highly effective when diagnosing bladder implantation. Ultrasound is preferred over MRI because it is more convenient and more affordable.Among them, the tramline sign “fully” obliterated was a new and reliable US sign for detecting bladder involvement.

### Acknowledgements

The researchers appreciate the help from the obstetrics and gynecology department and Department of Radiology at the First Affiliated Hospital of Anhui Medical University during data collection.

### Author contributions

XFS was responsible for the study design, proposal writing, data collection, data analysis, and initial drafting of the paper. TTZ and HWL view the MRI images and provide the image data. CFG and XFS view the US images and provide the us image data. YFY and XFS was responsible for the clinical and surgical data collection. CFG, HQZ, YL and WY contributed to data analysis. CXZ provided technical and material support, and revised subsequent drafts of the paper. as well as a critical review of the intellectual content of the article. All authors reviewed and approved the final manuscript.

### Funding

This work was supported by the Research fund Project of Anhui institute of Translational Medicine (2021zhyx-C35).

### Data availability

The datasets used and analysed during the current study are available from the corresponding author on reasonable request.

### Declarations

#### Human ethics and consent to participate

Not applicable.

#### Competing interests

The authors declare no competing interests.

#### Author details

<sup>1</sup>Department of Ultrasound, The First Affiliated Hospital of Anhui Medical University, Hefei 230022, China

<sup>2</sup>Department of Radiology, The First Affiliated Hospital of Anhui Medical University, Hefei, China

<sup>3</sup>Department of Obstetrics and Gynecology, The First Affiliated Hospital of Anhui Medical University, Hefei, China

Received: 19 June 2024 / Accepted: 19 November 2024

Published online: 26 November 2024

### References

1. Jauniaux E, Chantraine F, Silver RM, Langhoff-Roos J. Figo consensus guidelines on placenta accreta spectrum disorders: epidemiology. *Int J Gynecol Obstet.* 2018;140:265–73. <https://doi.org/10.1002/ijgo.12407>. DOI.
2. Luke RK, Sharpe JW, Greene RR. Placenta accreta: the adherent or invasive placenta. *Am J Obstet Gynecol.* 1966;95:660–8. [https://doi.org/10.1016/s0002-9378\(16\)34741-x](https://doi.org/10.1016/s0002-9378(16)34741-x).
3. Jauniaux E, Ayres-De-Campos D, Langhoff-Roos J, Fox KA, Collins S. Figo classification for the clinical diagnosis of placenta accreta spectrum disorders. *Int J Gynecol Obstet.* 2019;146:20–4. <https://doi.org/10.1002/ijgo.12761>.
4. Fitzpatrick KE, Sellers S, Spark P, Kurinczuk JJ, Brocklehurst P, Knight M. Incidence and risk factors for placenta accreta/increta/percreta in the UK: a national case-control study. *PLoS ONE.* 2012;7:e52893DOI. <https://doi.org/10.1371/journal.pone.0052893>.

5. Gielchinsky Y, Rojansky N, Fasouliotis SJ, Ezra Y. Placenta accreta—summary of 10 years: a survey of 310 cases. *Placenta*. 2002;23:210–4. <https://doi.org/10.1053/plac.2001.0764>.
6. Tadayon M, Javadifar N, Dastoorpoor M, Shahbazian N. Frequency, risk factors, and pregnancy outcomes in cases with placenta accreta spectrum disorder: a case-control study. *J Reprod Infertil*. 2022;23:279–87. <https://doi.org/10.18502/jri.v23i4.10814>. DOI.
7. You H, Wang Y, Han R, Gu J, Zeng L, Zhao Y. Risk factors for placenta accreta spectrum without prior cesarean section: a case-control study in China. *Int J Gynecol Obstet*. 2024;166:1092–9. <https://doi.org/10.1002/ijgo.15493>. DOI.
8. Jauniaux E, Bunce C, Grønbeck L, Langhoff-Roos J. Prevalence and main outcomes of placenta accreta spectrum: a systematic review and meta-analysis. *Am J Obstet Gynecol*. 2019;221:208–18. <https://doi.org/10.1016/j.jog.2019.01.233>. DOI.
9. Hobson SR, Kingdom JC, Murji A, Windrim RC, Carvalho JCA, Singh SS, Ziegler C, Birch C, Frecker E, Lim K, Cargill Y, Allen LM. 383-screening, diagnosis, and management of placenta accreta spectrum disorders. *J Obstet Gynaecol Can*. 2019;41:1035–49. <https://doi.org/10.1016/j.jogc.2018.12.004>. DOI.
10. Ishibashi H, Miyamoto M, Iwahashi H, Matsura H, Kakimoto S, Sakamoto T, Hada T, Takano M. Criteria for placenta accreta spectrum in the international federation of gynaecology and obstetrics classification, and topographic invasion area are associated with massive hemorrhage in patients with placenta previa. *Acta Obstet Gynecol Scand*. 2021;100:1019–25. <https://doi.org/10.1111/aogs.14143>. DOI.
11. Silver RM, Landon MB, Rouse DJ, Leveno KJ, Spong CY, Thom EA, Moawad AH, Caritis SN, Harper M, Wapner RJ, Sorokin Y, Miodovnik M, Carpenter M, Peaceman AM, O'Sullivan MJ, Sibai B, Langer O, Thorp JM, Ramin SM, Mercer BM. Maternal morbidity associated with multiple repeat cesarean deliveries. *Obstet Gynecol*. 2006;107:1226–DOI1232. <https://doi.org/10.1097/01.AOG.00219750.79480.84>.
12. Balayla J, Bondarenko HD. Placenta accreta and the risk of adverse maternal and neonatal outcomes. *J Perinat Med*. 2013;41:141–9. <https://doi.org/10.1515/jpm-2012-0219>. DOI.
13. Tillu N, Savalia A, Patwardhan S, Patil B. Placenta percreta with bladder invasion: the armamentarium available in its management. *Urol Annals*. 2019;11:324–7. [https://doi.org/10.4103/UA.UA\\_84\\_18](https://doi.org/10.4103/UA.UA_84_18). DOI.
14. Jariyawattanarat W, Thiravit S, Suvannareng V, Srisajjakul S, Sutthritpongsa P. Bladder involvement in placenta accreta spectrum disorder with placenta previa: mri findings and outcomes correlation. *Eur J Radiol*. 2023;160:110695DOI. <https://doi.org/10.1016/j.ejrad.2023.110695>.
15. Abbas F, Talati J, Wasti S, Akram S, Ghaffar S, Qureshi R. Placenta percreta with bladder invasion as a cause of life threatening hemorrhage. *J Urol*. 2000;164:1270–4.
16. Shamshirsaz AA, Fox KA, Salmanian B, Diaz-Arrastia CR, Lee W, Baker BW, Ballas J, Chen Q, Van Veen TR, Javadian P, Sangi-Haghpeykar H, Zacharias N, Welyt S, Cassidy CI, Moaddab A, Popek EJ, Hui SK, Teruya J, Bandi V, Coburn M, Cunningham T, Martin SR, Belfort MA. Maternal morbidity in patients with morbidly adherent placenta treated with and without a standardized multidisciplinary approach. *Am J Obstet Gynecol*. 2015;212:211–DOI218. <http://doi.org/10.1016/j.ajog.2014.08.019>.
17. Cali G, Foti F, Minneci G. Crystal Vue technology in the study of the uterine–bladder interface in a case of abnormally invasive placenta. *Donald School J Ultrasound Obstet Gynecol*. 2017;11:177–8. <https://doi.org/10.5005/jp-journal-1519>. DOI.
18. Shijing SM, Qingqing WM, Jingjing WM, Jinghua LM, Dan YM. Clinical applications of crystal vue technology: a review. *Adv Ultrasound Diagnosis Therapy*. 2022;6:1–6. <https://doi.org/10.37015/AUDT.2021.200067>. DOI.
19. Shih JC, Palacios JJ, Su YN, Shyu MK, Lin CH, Lin SY, Lee CN. Role of three-dimensional power doppler in the antenatal diagnosis of placenta accreta: comparison with gray-scale and color doppler techniques. *Ultrasound Obstet Gynecol*. 2009;33:193–203. <https://doi.org/10.1002/uog.6284>. DOI.
20. Dall'Asta A, Paramasivam G, Lees CC. Qualitative evaluation of crystal vue rendering technology in assessment of fetal lip and palate. *Ultrasound Obstet Gynecol*. 2017;49:549–52. <https://doi.org/10.1002/uog.17346>. DOI.
21. Adu-Bredu TK, Ridwan R, Aditiawarman A, Ariani G, Collins SL, Aryananda RA. Three-dimensional volume rendering ultrasound for assessing placenta accreta spectrum severity and discriminating it from simple scar dehiscence. *Amer J Obstet Gynecol Mfm*. 2024;6:101321DOI. <https://doi.org/10.1016/j.ajogmf.2024.101321>.
22. Bourgioti C, Zafeiropoulou K, Fotopoulos S, Nikolaidou ME, Antoniou A, Tzavara C, Mouloupoulos LA. Mri features predictive of invasive placenta with extrauterine spread in high-risk gravid patients: a prospective evaluation. *Am J Roentgenol*. 2018;211:701–11. <https://doi.org/10.2214/AJR.17.19303>. DOI.
23. D'Antonio F, Iacovella C, Palacios-Jaraquemada J, Bruno CH, Manzoli L, Bhide A. Prenatal identification of invasive placentation using magnetic resonance imaging: systematic review and meta-analysis. *Ultrasound Obstet Gynecol*. 2014;44:8–16. <https://doi.org/10.1002/uog.13327>. DOI.
24. Kumar I, Verma A, Ojha R, Shukla RC, Jain M, Srivastava A. Invasive placental disorders: a prospective us and mri comparative analysis. *Acta Radiol*. 2017;58:121–8. <https://doi.org/10.1177/0284185116638567>. DOI.
25. Chen X, Shan R, Song Q, Wei X, Liu W, Wang G. Placenta percreta evaluated by mri: correlation with maternal morbidity. *Arch Gynecol Obstet*. 2020;301:851–7. <https://doi.org/10.1007/s00404-019-05420-5>. DOI.
26. Barzily E, Brandt B, Gilboa Y, Kassif E, Achiron R, Raviv-Zilka L, Katorza E. Comparative analysis of ultrasound and mri in the diagnosis of placenta accreta spectrum. *J Matern -Fetal Neonatal Med*. 2022;35:4056–9. <https://doi.org/10.1080/14767058.2020.1846699>. DOI.
27. Dall'Asta A, Forlani F, Shah H, Paramasivam G, Yazbek J, Bourne T, Cali G, Lees C. Evaluation of the tramline sign in the prediction of placenta accreta spectrum and perioperative outcomes in anterior placenta previa. *Ultraschall Med*. 2022;43:e118–24. <https://doi.org/10.1055/a-1309-1665>. DOI.
28. Xin S, Wan H, Zeng X, Fu Y, Wang Z, Lai H, Xiong Y, Zheng J, Liu L. Early warning model of placenta accreta spectrum disorders complicated with cervical implantation: a single-center retrospective study. *J Healthc Eng*. 2022;2022:1–7. <https://doi.org/10.1155/2022/8128689>.
29. Palacios-Jaraquemada JM, Nieto-Calvache A, Aryananda RA, Basanta N. Placenta accreta spectrum into the parametrium, morbidity differences between upper and lower location. *J Matern -Fetal Neonatal Med*. 2023;36:2183764DOI. <https://doi.org/10.1080/14767058.2023.2183764>.
30. Jauniaux E, Bhide A, Kennedy A, Woodward P, Hubinont C, Collins S. Figo consensus guidelines on placenta accreta spectrum disorders: prenatal diagnosis and screening. *Int J Gynecol Obstet*. 2018;140:274–80. <https://doi.org/10.1002/ijgo.12408>. DOI.
31. Collins SL, Ashcroft A, Braun T, Calda P, Langhoff-Roos J, Morel O, Stefanovic V, Tutschek B, Chantraine F. Proposal for standardized ultrasound descriptors of abnormally invasive placenta (aip). *Ultrasound Obstet Gynecol*. 2016;47:271–5. <https://doi.org/10.1002/uog.14952>. DOI.
32. Chen S, Chen Q, Du X, Chen S, Li W, Chen S. Value of crystal vue technique in detecting the placenta accreta spectrum located in c-section scar area. *Med Ultrason*. 2020;22:438–44. <https://doi.org/10.11152/mu-2578>. DOI.
33. Poder L, Weinstein S, Maturen KE, Feldstein VA, Mackenzie DC, Oliver ER, Shipp TD, Strachowski LM, Sussman BL, Wang EY, Weber TM, Whitcomb BP, Glanc P. Acr appropriateness criteria® placenta accreta spectrum disorder. *J Am Coll Radiol*. 2020;17:5207–14. <https://doi.org/10.1016/j.jacr.2020.01.031>. DOI.
34. Morel O, Collins SL, Uzan-Augui J, Masselli G, Duan J, Chabot-Lecoanet AC, Braun T, Langhoff-Roos J, Soyer P, Chantraine F. A proposal for standardized magnetic resonance imaging (mri) descriptors of abnormally invasive placenta (aip) – from the international society for aip. *Diagn Interv Imaging*. 2019;100:319–25. <https://doi.org/10.1016/j.diii.2019.02.004>. DOI.
35. Liu CN, Yu FB, Xu YZ, Li JS, Guan ZH, Sun MN, Liu CA, He F, Chen DJ. Prevalence and risk factors of severe postpartum hemorrhage: a retrospective cohort study. *Bmc Pregnancy Childbirth*. 2021;21:332DOI. <https://doi.org/10.1186/s12884-021-03818-1>.
36. Ali H, Chandrarahan E. Etiopathogenesis and risk factors for placental accreta spectrum disorders. *Best Pract Res Clin Obstet Gynaecol*. 2021;72:4–12. <https://doi.org/10.1016/j.bpobgyn.2020.07.006>. DOI.
37. Jauniaux E, Bhide A. Prenatal ultrasound diagnosis and outcome of placenta previa accreta after cesarean delivery: a systematic review and meta-analysis. *Am J Obstet Gynecol*. 2017;217:27–36. <https://doi.org/10.1016/j.ajog.2017.02.050>. DOI.
38. Timor-Tritsch IE, Monteagudo A, Cali G, Vintzileos A, Viscarello R, Al-Khan A, Zamudio S, Mayberry P, Cordoba MM, Dar P. Cesarean scar pregnancy is a precursor of morbidly adherent placenta. *Ultrasound Obstet Gynecol*. 2014;44:346–53. <https://doi.org/10.1002/uog.13426>. DOI.
39. Bhatia A, Palacio M, Wright AM, Yeo G. Lower uterine segment scar assessment at 11–14 weeks' gestation to screen for placenta accreta spectrum in women with prior cesarean delivery. *Ultrasound Obstet Gynecol*. 2022;59:40–8. <https://doi.org/10.1002/uog.23734>.
40. Allen L, Jauniaux E, Hobson S, Papillon-Smith J, Belfort MA. Figo consensus guidelines on placenta accreta spectrum disorders: nonconservative surgical management. *Int J Gynecol Obstet*. 2018;140:281–90. <https://doi.org/10.1002/ijgo.12409>. DOI.

41. Tam TK, Dozier J, Martin JJ. Approaches to reduce urinary tract injury during management of placenta accreta, increta, and percreta: a systematic review. *J Matern -Fetal Neonatal Med.* 2012;25:329–34. <https://doi.org/10.3109/14767058.2011.576720>. DOI.
42. O'Brien JM, Barton JR, Donaldson ES. The management of placenta percreta: conservative and operative strategies. *Am J Obstet Gynecol.* 1996;175:1632–8. [https://doi.org/10.1016/s0002-9378\(96\)70117-5](https://doi.org/10.1016/s0002-9378(96)70117-5). DOI.
43. Sentilhes L, Kayem G, Chandraran E, Palacios-Jaraquemada J, Jauniaux E. Figo consensus guidelines on placenta accreta spectrum disorders: conservative management. *Int J Gynecol Obstet.* 2018;140:291–8. <https://doi.org/10.1002/ijgo.12410>. DOI.
44. Giuseppe C, Salvatore P, Federica C, Francesco L, Francesco D, Alessandro L, Gloria C. Urinary tract injuries during surgery for placenta accreta spectrum disorders. *Eur J Obstet Gynecol Reprod Biol.* 2023;287:93–6. <https://doi.org/10.1016/j.ejogrb.2023.05.036>. DOI.
45. Peng Y, Jiang L, Peng C, Wu D, Chen L. The application of prophylactic balloon occlusion of the internal iliac artery for the treatment of placenta accreta spectrum with placenta previa: a retrospective case-control study. *Bmc Pregnancy Childbirth.* 2020;20:349DOI. <https://doi.org/10.1186/s12884-020-3041-4>.
46. Silver RM, Fox KA, Barton JR, Abuhamad AZ, Simhan H, Huls CK, Belfort MA, Wright JD. Center of excellence for placenta accreta. *Am J Obstet Gynecol.* 2015;212:561–8. <https://doi.org/10.1016/j.ajog.2014.11.018>. DOI.
47. Norris BL, Everaerts W, Posma E, Murphy DG, Umstad MP, Costello AJ, Wrede CD, Kearsley J. The urologist's role in multidisciplinary management of placenta percreta. *Bju Int.* 2016;117:961–5. <https://doi.org/10.1111/bju.13332>. DOI.
48. Konijeti R, Rajfer J, Askari A. Placenta percreta and the urologist. *Rev Urol.* 2009;11:173–6.
49. Shih JC, Kang J, Tsai SJ, Lee JK, Liu KL, Huang KY. The rail sign: an ultrasound finding in placenta accreta spectrum indicating deep villous invasion and adverse outcomes. *Am J Obstet Gynecol.* 2021;225:291–2. <https://doi.org/10.1016/j.ajog.2021.03.018>. DOI.
50. Jauniaux E, Collins S, Burton GJ. Placenta accreta spectrum: pathophysiology and evidence-based anatomy for prenatal ultrasound imaging. *Am J Obstet Gynecol.* 2018;218:75–87. <https://doi.org/10.1016/j.ajog.2017.05.067>. DOI.
51. Chantraine F, Collins SL. Prenatal ultrasound imaging for placenta accreta spectrum (pas): a practical guide. *Curr Obstet Gynecol Rep.* 2019;8:86–93. <https://doi.org/10.1007/s13669-019-00267-8>. DOI.
52. Adu-Bredu TK, Collins SL, Nieto-Calvache AJ. Ultrasound discrimination between placenta accreta spectrum and urinary bladder varices. *Aust N Z J Obstet Gynaecol.* 2023;63:725–7. <https://doi.org/10.1111/ajo.13703>. DOI.
53. Maynard H, Zamudio S, Jauniaux E, Collins SL. The importance of bladder volume in the ultrasound diagnosis of placenta accreta spectrum disorders. *Int J Gynecol Obstet.* 2018;140:332–7. <https://doi.org/10.1002/ijgo.12370>. DOI.
54. Thiravit S, Ma K, Goldman I, Chanprapaph P, Jha P, Hippe DS, Dighe M. Role of ultrasound and mri in diagnosis of severe placenta accreta spectrum disorder: an intraindividual assessment with emphasis on placental bulge. *Am J Roentgenol.* 2021;217:1377–88. <https://doi.org/10.2214/AJR.21.25581>. DOI.
55. Jha P, Rabban J, Chen LM, Goldstein RB, Weinstein S, Morgan TA, Shum D, Hills N, Ohliger MA, Poder L. Placenta accreta spectrum: value of placental bulge as a sign of myometrial invasion on mr imaging. *Abdom Radiol.* 2019;44:2572–81. <https://doi.org/10.1007/s00261-019-02008-0>. DOI.
56. Al-Khan A, Alshowaikh K, Krishnamoorthy K, Saber S, Alvarez M, Pappas L, Mannion C, Kayaalp E, Francis A, Alvarez-Perez J. Pulsatile vessel at the posterior bladder wall: a new sonographic marker for placenta percreta. *J Obstet Gynaecol Res.* 2022;48:1149–56. <https://doi.org/10.1111/jog.15208>. DOI.
57. Masselli G, Brunelli R, Casciani E, Polettoni E, Piccioni MG, Anceschi M, Gualdi G. Magnetic resonance imaging in the evaluation of placental adhesive disorders: correlation with color doppler ultrasound. *Eur Radiol.* 2008;18:1292–9. <https://doi.org/10.1007/s00330-008-0862-8>. DOI.
58. Palacios-Jaraquemada JM, Bruno CH, Martin E. Mri in the diagnosis and surgical management of abnormal placentation. *Acta Obstet Gynecol Scand.* 2013;92:392–7. <https://doi.org/10.1111/j.1600-0412.2012.01527.x>. DOI.

## Publisher's note

Springer Nature remains neutral with regard to jurisdictional claims in published maps and institutional affiliations.